TU/e EINDHOVEN UNIVERSITY OF TECHNOLOGY

Effects of DC-Field Excitation on the Incremental Inductance of a Variable Flux Reluctance Machine

Citation for published version (APA):
Ceylan, D., Friedrich, L. A. J., Boynov, K. O., & Lomonova, E. A. (2021). Effects of DC-Field Excitation on the Incremental Inductance of a Variable Flux Reluctance Machine. *IEEE Transactions on Magnetics*, *57*(2), Article 9162149. https://doi.org/10.1109/TMAG.2020.3015093

Document license:
TAVERNE

DOI:
10.1109/TMAG.2020.3015093

Document status and date:
Published: 01/02/2021

Document Version:
Publisher's PDF, also known as Version of Record (includes final page, issue and volume numbers)

Please check the document version of this publication:

• A submitted manuscript is the version of the article upon submission and before peer-review. There can be important differences between the submitted version and the official published version of record. People interested in the research are advised to contact the author for the final version of the publication, or visit the DOI to the publisher's website.
• The final author version and the galley proof are versions of the publication after peer review.
• The final published version features the final layout of the paper including the volume, issue and page numbers.

Link to publication

General rights
Copyright and moral rights for the publications made accessible in the public portal are retained by the authors and/or other copyright owners and it is a condition of accessing publications that users recognise and abide by the legal requirements associated with these rights.

• Users may download and print one copy of any publication from the public portal for the purpose of private study or research.
• You may not further distribute the material or use it for any profit-making activity or commercial gain
• You may freely distribute the URL identifying the publication in the public portal.

If the publication is distributed under the terms of Article 25fa of the Dutch Copyright Act, indicated by the "Taverne" license above, please follow below link for the End User Agreement:

www.tue.nl/taverne

Take down policy
If you believe that this document breaches copyright please contact us at:

openaccess@tue.nl

providing details and we will investigate your claim.

Download date: 05. Oct. 2023

Effects of DC-Field Excitation on the Incremental Inductance of a Variable Flux Reluctance Machine

D. Ceylan, L. A. J. Friedrich, K. O. Boynov, and E. A. Lomonova

Department of Electrical Engineering, Eindhoven University of Technology, 5612 Eindhoven, The Netherlands

This article presents a method for the computation of the incremental inductances in a 12/10 variable flux reluctance machine (VFRM) using the hybrid analytical modeling coupled with a fixed-point nonlinear solver. The variation of incremental and apparent inductance with respect to the dc-field excitation is investigated for both zero and non-zero ac-field excitations. The results show that the difference between both inductance values is not negligible after 25 A/mm^2 dc-current density for the investigated benchmark without the ac field. Moreover, when a non-zero ac field is introduced in addition to the dc-field, the apparent inductance becomes misleading not only under magnetic saturation but also under low excitation in the linear region of the saturation curve. The results obtained with the proposed nonlinear hybrid model are compared with the finite element method in terms of magnetic flux density distribution and incremental inductance value. The root-mean-square discrepancy of magnetic flux density distribution is found to be 37.6 mT. Furthermore, the discrepancy between incremental inductance results of the proposed method and the finite element model is calculated as 1.43%, while the proposed approach requires less post-processing and necessitates ten times less number of degrees-of-freedom.

Index Terms— **Fixed-point method (FPM), hybrid analytical modeling (HAM), incremental inductance, variable flux reluctance machines (VFRMs).**

I. Introduction

THE accurate calculation of winding inductance in electrical machines is critical to achieve the optimum design and control. One of the common mistakes done by engineers in the field of electromechanics is using apparent inductance instead of incremental under the magnetic saturation. While the apparent inductance is defined as the ratio of the flux linkage to the excitation current, the incremental inductance is a partial derivative of the flux linkage with respect to the excitation current [1]. Wang and Lin [2] proposed an analytical method to estimate the incremental inductance of a permanent magnet (PM) machine. An experimental procedure to obtain the incremental inductance profile of a switch reluctance machine is presented in [3]. Due to the fact that the difference between these two inductance values increases with magnetic saturation of the iron material, the accurate calculation of incremental inductance becomes critical for electrical machines operating under the magnetic saturation such as variable flux reluctance machine (VFRM). VFRM has both dc- and ac-field windings in its stator, while it exhibits a doubly salient rotor and stator structure as explained in [4]. The cost of VFRM is relatively low because of its PM-free structure. In addition, VFRM has improved flux weakening capability to increase the efficiency at high speed [5]. Besides, since the identical field windings on each pole provide identical flux path for each phase, VFRM has more sinusoidal flux linkage and back electromotive force under heavy magnetic saturation compared to the other salient machines such as doubly fed doubly salient and doubly salient PM machines as discussed in [6]. In order to use the advantage of having sinusoidal waveforms, VFRM performs under saturation. Therefore, the incremental inductance of a VFRM deviates from its apparent inductance during the excitation which makes the accurate calculation of the incremental inductance critical.

The finite element method (FEM) is the most commonly used method to simulate electrical machines including nonlinear properties since there exist several commercial packages able to automate numerical modeling and computation. Incremental analysis of a transformer is presented in [7] using FEM. However, the calculation of incremental inductance with FEM requires extra post-processing to obtain the derivative of flux linkage with respect to the excitation current. The requirement of post-processing and a large number of mesh elements in the airgap are two main factors increasing the computational cost of incremental inductance calculation using FEM.

The hybrid analytical modeling (HAM) technique is used to calculate the magnetic field distribution of a VFRM in this study. As explained in [8], HAM uses magnetic equivalent circuit (MEC) theory in both stator and rotor. Unlike FEM, the magnetic field in the airgap is modeled analytically using Fourier analysis (FA) in HAM. In addition, HAM can use a coarser mesh than FEM in the stator and rotor because MEC is an integral method, while FEM is differential. Therefore, HAM with mesh-free airgap and integral MEC is advantageous compared to FEM in terms of computational time [9]. Moreover, the nonlinear magnetic properties of iron material are included using the fixed-point method (FPM). As discussed in [10], FPM locally linearizes the nonlinear saturation curve using tangent lines. In order to model the magnetic saturation, an additional source of magneto-motive force (MMF) is introduced as a function of intercept and slope of tangent lines, which are called remanent flux and incremental permeability, respectively. Since the saturation-related MMF source is decoupled from other current or PM sources, incremental inductance can be calculated without

Manuscript received May 7, 2020; revised July 27, 2020; accepted August 4, 2020. Date of publication August 7, 2020; date of current version January 20, 2021. Corresponding author: D. Ceylan (e-mail: d.ceylan@tue.nl).

Color versions of one or more of the figures in this article are available online at https://ieeexplore.ieee.org.

Digital Object Identifier 10.1109/TMAG.2020.3015093

0018-9464 © 2020 IEEE. Personal use is permitted, but republication/redistribution requires IEEE permission.
See https://www.ieee.org/publications/rights/index.html for more information.

Authorized licensed use limited to: Eindhoven University of Technology. Downloaded on September 01,2021 at 08:01:42 UTC from IEEE Xplore. Restrictions apply.

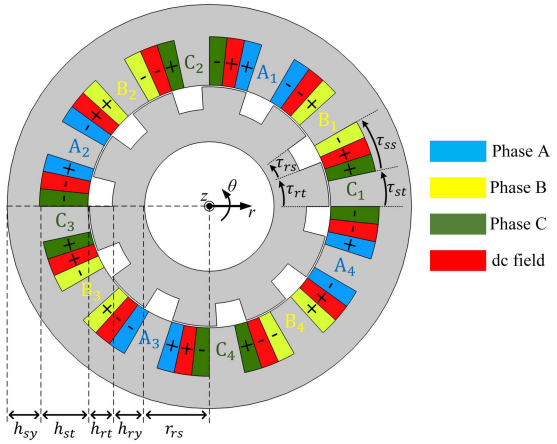

Fig. 1. 2-D benchmark of a 12/10 variable flux reluctance machine (VFRM) machine.

TABLE I
BENCHMARK DIMENSIONS

h_{sy}	h_{st}	h_{rt}	h_{ry}	h_{rs}	$\frac{\tau_{rs}}{\tau_{rt}}$	$\frac{\tau_{ss}}{\tau_{st}}$
10 mm	15 mm	7 mm	10 mm	20 mm	0.4	0.6

computing the derivative of flux linkage as discussed in [11]. Hence, the proposed approach requires less computational effort to calculate incremental inductance than FEM.

In this article, effects of dc-field excitation on the incremental inductance of a VFRM is analyzed using HAM coupled with FPM nonlinear solver. The difference between apparent and incremental inductances is observed for zero and nonzero ac-field excitation. The results are compared with FEM results.

II. BENCHMARK

A 12/10 VFRM given in Fig. 1 is selected as benchmark. It has concentrated ac- and dc-field windings in the stator. In the given winding configuration, each phase has four series-connected windings. Dimensions of the benchmark are given in Table I. While the stack length of the benchmark in z-direction is 0.2 m, the airgap is selected as 1 mm. The soft-magnetic material is selected as Cogent M800, which exhibits a nonlinear B–H characteristic.

III. MODELING METHOD

The apparent and incremental inductances of the analyzed benchmark are calculated using two different modeling methods: FEM and HAM. HAM uses a strong coupling between MEC and FA techniques to calculate magnetic field distribution. The model parameters of HAM and FEM are selected implementing a sensitivity analysis for each of them. In the stator and rotor of HAM, 8600 MEC elements are used in total, each of which has four annular sector-shaped reluctance elements in both θ- and r-directions. The number of harmonics included in the FA of the airgap flux is 50, which results in 200 Fourier coefficients. A Dirichlet boundary condition is introduced at the outer radius of the stator for

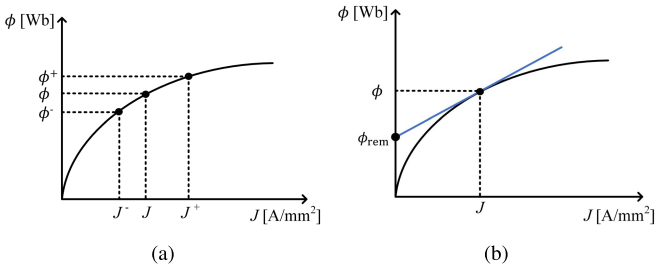

Fig. 2. Different incremental computations in FEM and HAM. (a) FEM. (b) HAM.

both models. Moreover, quadratic triangular mesh elements are used in FEM. The number of layers used in the airgap is selected as four which results in totally 42 700 elements in the benchmark. Consequently, the number of degrees-of-freedom of the hybrid analytical model is 8800, while the finite element model has 85 601 degrees-of-freedom.

Since the implementation of HAM is explained in [8] and [12] in detail, it is not discussed in this article. Moreover, the nonlinear solver of the hybrid analytical model is developed using FPM. This method linearizes the nonlinear saturation curve using tangent lines for each mesh element in the reluctance network of the stator and rotor. After the linearization, tangent lines are expressed as

$$H = \frac{B}{\mu_0 \mu_r} - \frac{B_r}{\mu_0 \mu_r} \tag{1}$$

where H is the magnetic field strength, B is the magnetic flux density, μ_0 is the permeability of free-space, μ_r is the incremental relative permeability which is defined as the slope of the tangent line, and B_r is the remanent flux density which is the intercept of the tangent line. The term with B_r in (1) is considered as the equivalent magnetization of the soft-magnetic material, and it is included in the model as an additional MMF source as discussed in [13]. Values of B, μ_r, and B_r are updated in each iteration of FPM using the nonlinear B–H characteristics of the electrical steel and the developed hybrid analytical model. While μ_r and B_r are calculated using tangent lines on the points where B results of HAM are located, HAM takes μ_r and B_r and returns a new B-field distribution. In addition, μ_r and B_r of tangent lines are used in the reluctance and MMF source distributions of HAM. For the convergence criterion, the relative difference of the magnetic flux density distribution between successive iterations is used. If the relative difference

$$\varepsilon_B^{(i)} = \frac{||B^{(i)} - B^{(i-1)}||}{||B^{(i)}||} \tag{2}$$

is smaller than 0.1%, FPM stops the iteration.

IV. INDUCTANCE CALCULATION

A. Apparent Inductance

The calculation of apparent inductance, L_{app}, using FEM or HAM does not require other computations than the

Authorized licensed use limited to: Eindhoven University of Technology. Downloaded on September 01,2021 at 08:01:42 UTC from IEEE Xplore. Restrictions apply.

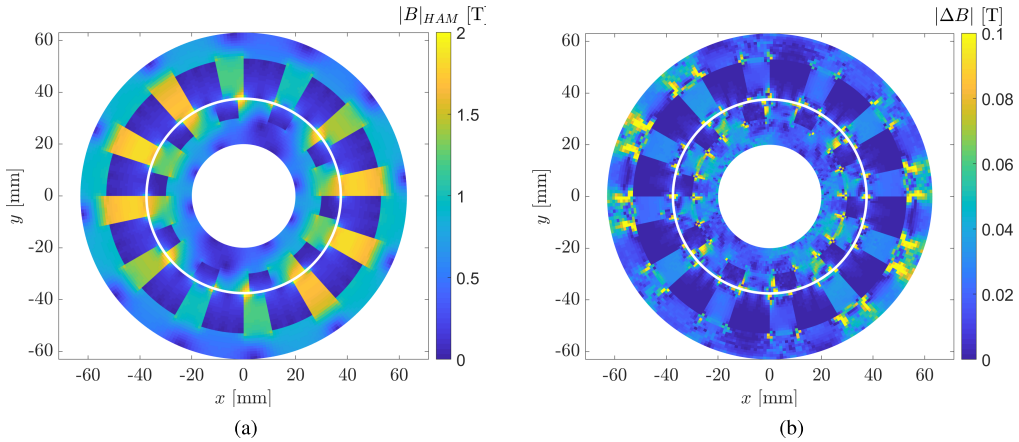

Fig. 3. Flux density distribution calculated using HAM and the difference between FEM and HAM results. (a) HAM. (b) Error.

flux linkage. It is defined as the ratio of the total flux linked by an ac-field winding to the dc-field excitation current

$$L_{\text{app}} = \frac{\lambda}{I_{\text{dc}}} = \frac{N\phi}{I_{\text{dc}}} \tag{3}$$

where λ is the total flux linkage, ϕ is the magnetic flux, N is the number of turns, and I_{dc} is the dc current.

The system of equations of HAM is solved for magnetic scalar potentials of the reluctance network defined in the stator and the rotor, and Fourier coefficients defined in the FA in the airgap. The magnetic flux density distributions in θ- and r-directions, B_θ and B_r, are calculated using these HAM outputs. Then, ϕ in (3) is expressed as a function of B_r for winding C_1 in Fig. 1

$$\phi = l_s \int_0^{\tau_{st}} r B_r(r,\theta) d\theta \tag{4}$$

where the radius, r, is evaluated at the stator tooth opening. Each winding given in Fig. 1 has its own boundaries for the line integration in (4) depending on its position. In addition, in HAM, the winding related MMF sources are defined in terms of dc- and ac-current densities, J_{dc} and J_{ac}. Hence, I_{dc} in (3) is expressed as

$$I_{\text{dc}} = \frac{J_{\text{dc}} S_{\text{dc}}}{N} \tag{5}$$

where S_{dc} is the area of the dc-field winding on the stator slot surface. Using (3)–(5), the expression for apparent inductance to be used in HAM is found as

$$L_{\text{app}} = \frac{N^2 l_s}{J_{\text{dc}} S_{\text{dc}}} \int r B_r(r,\theta) d\theta. \tag{6}$$

B. Incremental Inductance

The incremental inductance, L_{inc}, is defined as a partial derivative of λ with respect to I_{dc}

$$L_{\text{inc}} = \frac{\partial \lambda}{\partial I_{\text{dc}}} = N \frac{\partial \phi}{\partial I_{\text{dc}}}. \tag{7}$$

The implementation of (7) with FEM is only possible in post-processing using either continuous or discrete derivative. For the continuous derivative, ϕ values calculated by FEM are interpolated as a function of I_{dc} which causes additional post-processing and therefore, computational effort

$$L_{\text{inc}}^{\text{spline}} = \frac{N^2}{S_{\text{dc}}} \frac{\partial f_\phi(J_{\text{dc}})}{\partial J_{\text{dc}}} \tag{8}$$

shows the calculation of incremental inductance using continuous derivative where f_ϕ is the spline interpolant of the magnetic flux. The discrete method approximates the partial derivate using the central finite difference method (FDM) as illustrated in Fig. 2(a), where J^+ and J^- are very close to J. Considering Fig. 2(a), the incremental inductance can be calculated in the post-processing of FEM using

$$L_{\text{inc}}^{\text{FDM}} = \frac{N^2}{S_{\text{dc}}} \frac{\phi^+ - \phi^-}{J_{\text{dc}}^+ - J_{\text{dc}}^-}. \tag{9}$$

However, FEM calculations are repeated two times more for the operating current densities J^+ and J^- which increases the total simulation time. Unlike FEM, FPM used in HAM does not require an extensive post-processing for the incremental analysis of inductance. The advantage of FPM is that MMF sources related to magnetic saturation, $\mathcal{F}_{\text{sat}}$, and other field windings, $\mathcal{F}_{\text{dc}}$, $\mathcal{F}_{\text{ac}}$, are available in HAM separately

$$\mathcal{F} = \mathcal{F}_{\text{dc}} + \mathcal{F}_{\text{ac}} + \mathcal{F}_{\text{sat}}. \tag{10}$$

After convergence of the FPM algorithm, the total flux linkage, λ, and the converged values of μ_r and B_{rem} for each mesh element are found. Then, $\mathcal{F}_{\text{dc}}$ is set to zero without any change in other sources. The resulting HAM matrix is inverted one more time without FPM with resultant μ_r and B_{rem} values under the excitation of $\mathcal{F}_{\text{ac}}$ and $\mathcal{F}_{\text{sat}}$. The flux linkage result of this HAM calculation is called remanent flux linkage, λ_{rem}, which is the intercept of the tangent line given in Fig. 2(b). After the last linear HAM calculation, incremental inductance is obtained using

$$L_{\text{inc}}^{\text{HAM}} = \frac{N^2(\phi - \phi_{\text{rem}})}{J_{\text{dc}} S_{\text{dc}}}. \tag{11}$$

In addition, it should be noted that the developed 2-D models ignore the end-windings which decreases the flux inkage. Therefore, 2-D approximation gives relatively lower apparent inductance values than 3-D for the same excitation current.

Authorized licensed use limited to: Eindhoven University of Technology. Downloaded on September 01,2021 at 08:01:42 UTC from IEEE Xplore. Restrictions apply.

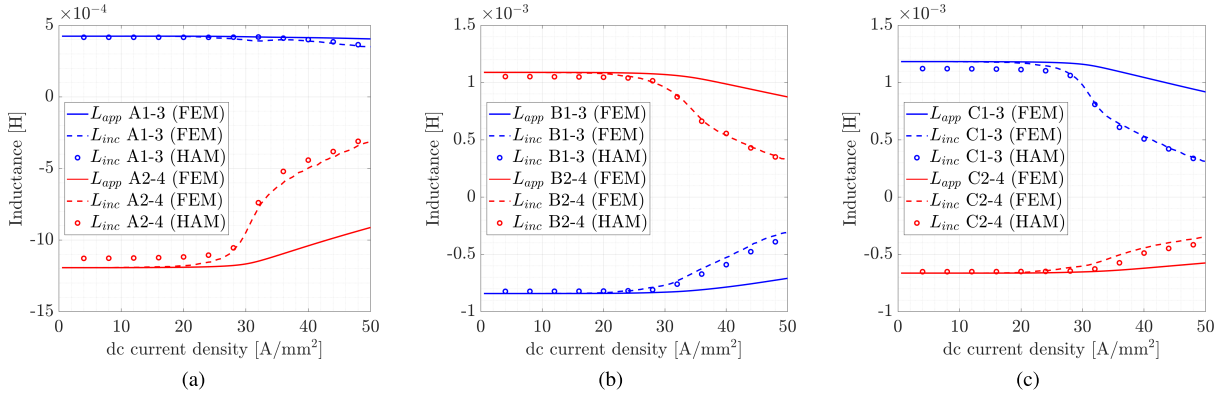

Fig. 4. Effect of dc-field excitation on apparent and incremental inductances for zero ac-field excitation. (a) Phase A. (b) Phase B. (c) Phase C.

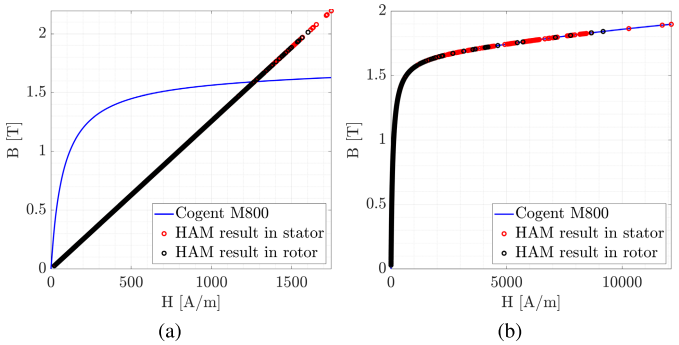

Fig. 5. Initial (a) and final (b) magnetic flux density distributions calculated by HAM compared to the saturation curve of Cogent M800 steel.

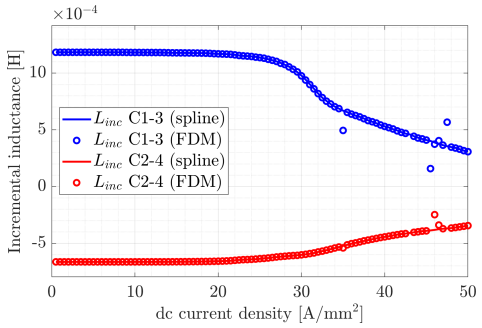

Fig. 6. Incremental inductance results of discrete (FDM) and continuous (spline) methods used in FEM.

However, this approximation affects the incremental inductance less than apparent, because the flux linkage contribution of the end-windings does not change the partial derivative of the flux linkage with respect to the current.

V. Results

The benchmark of Fig. 1 is analyzed using the developed hybrid analytical and finite element models. A magnetostatic analysis is performed for the rotor position given in Fig. 1 using FEM and HAM. Comsol Multiphysics software is used for the FEM calculation. In order to verify the developed nonlinear hybrid analytical model coupled with FPM, the magnetic flux density distribution result of HAM is compared with FEM in Fig. 3 for 35 A/mm^2 dc-current density and zero ac-current density. Fig. 3(b) shows that the maximum local error is located at the corners of the teeth. It is because the gradient is ill-defined at a corner point and makes FEM calculation less accurate. The root-mean-square error of B-field result of HAM is calculated as 37.6 mT. Moreover, to observe the saturation level in HAM under the same excitation, the normalized magnetic flux density and magnetic field strength values of each mesh element in the stator and rotor are compared with the saturation curve of Cogent M800 steel in Fig. 5. It can be seen that while the permeability is assigned as 1000 in the initial stage, the final B and H results are located on the saturation curve after FPM iterations where some of them are in the deep saturation region.

After the verification of the developed hybrid analytical model, ac-field excitation is kept zero while J_{dc} is increased from zero to 50 A/mm^2. The number of turns is selected as 34 for each winding considering the maximum carrying current and American wire gauge standards. Resultant inductance variations with respect to J_{dc} are presented in Fig. 4 where the solid lines are apparent inductance, dashed lines, and dots are incremental inductance calculated by FEM with spline interpolation and HAM with FPM, respectively. The discrepancy between two incremental results is calculated as 1.43%. Moreover, it is shown that larger J_{dc} values than 25 A/mm^2 result in a difference between L_{inc} and L_{app} for winding A2–4, B2–4, and C1–3 where the magnetic flux density is higher, as shown in Fig. 3(a). In addition, continuous and discrete methods used to calculate L_{inc} in the post-processing of FEM are compared for phase C in Fig. 6. It is observed that FDM yields numerical errors due to discrete derivation.

Effect of dc-field excitation on incremental and apparent inductance is investigated also with the non-zero ac field. The peak value of ac-current density is selected as 5 A/mm^2. Considering the rotor position given in Fig. 1, the current density value of each phase is properly commutated. Fig. 7 shows that the apparent approximation becomes unrealistic with the non-zero ac-current source. The reason is that the ac component of flux linkage contributes to the total flux linkage as an offset considering the total flux linkage as a function of dc current. Moreover, the effect of saturation can be observed on L_{inc} after 22 A/mm^2. Lastly, the variations of apparent and incremental inductances of windings C_1 and C_3 are compared with respect to J_{dc} for 0, 5, and 10 A/mm^2 peak values of J_{ac} in Figs. 8 and 9.

Authorized licensed use limited to: Eindhoven University of Technology. Downloaded on September 01,2021 at 08:01:42 UTC from IEEE Xplore. Restrictions apply.

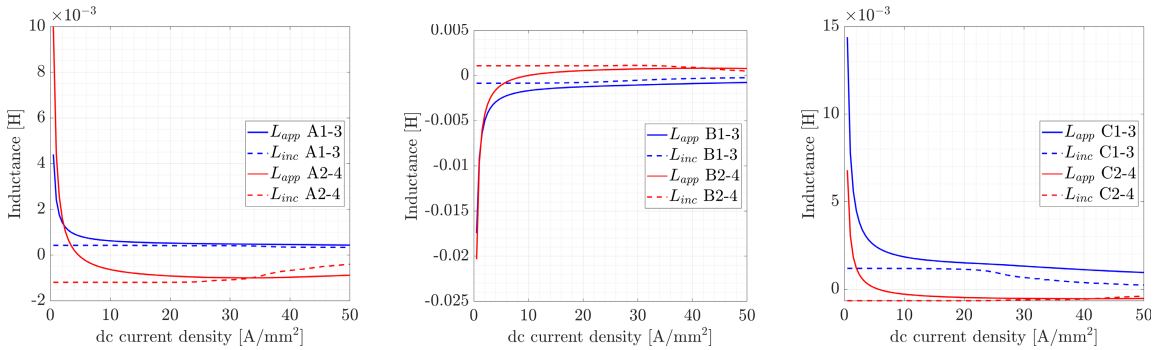

(a) (b) (c)

Fig. 7. Effect of dc-field excitation on apparent and incremental inductances for non-zero ac-field excitation. (a) Phase A. (b) Phase B. (c) Phase C.

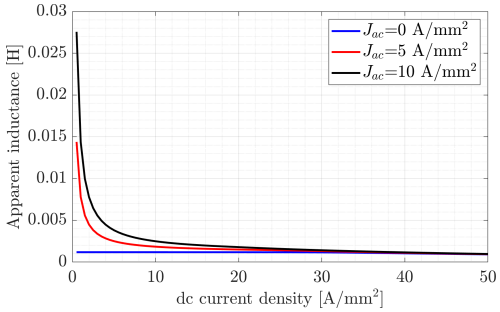

Fig. 8. Variation of apparent inductance with respect to dc-current density for different ac-field excitation levels.

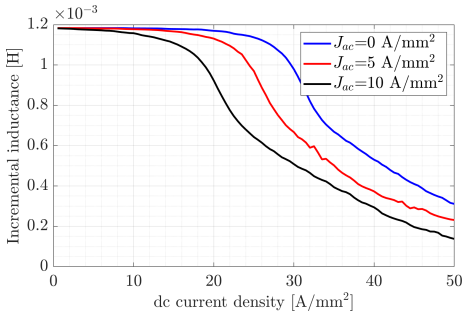

Fig. 9. Variation of incremental inductance with respect to dc-current density for different ac field excitation levels.

VI. Conclusion

The effect of dc-field excitation on the incremental and apparent inductance is investigated using FEM and HAM. It is shown that the proposed hybrid analytical model coupled with fixed-point nonlinear solver is able to compute the incremental analysis with more accuracy and less computational effort compared to FEM. The main two reasons of that are the mesh-free airgap of HAM and the fact that the winding and saturation related MMF sources are decoupled in FPM. A VFRM benchmark is investigated using the developed hybrid analytical model under different ac- and dc-field excitation levels. It is observed that increasing the dc-field excitation decreases apparent and incremental mutual inductances between ac- and dc-field windings after 25 A/mm^2 for the analyzed benchmark with non-zero ac-field due to the magnetic saturation. Furthermore, the apparent inductance gives unrealistically large values compared to the incremental inductances under the saturation or non-zero ac-field. Also, the magnetic flux density and inductance obtained by the proposed method demonstrate a good agreement with FEM results. The discrepancy between the incremental inductance results of the proposed model and FEM is equal to 1.43%.

Acknowledgment

This work was supported by Protonic Holland (https://www.protonic.nl/en/).

References

[1] X. Wang, P. Yi, Z. Zhou, Z. Sun, and W. Ruan, "Improvements in the permanent magnet synchronous motor torque model using incremental inductance," *IET Electr. Power Appl.*, vol. 14, no. 1, pp. 109–118, Jan. 2020.

[2] S.-J. Wang and S.-K. Lin, "Analytical prediction of the incremental inductance of the permanent magnet synchronous motors," *IEEE Trans. Magn.*, vol. 40, no. 4, pp. 2044–2046, Jul. 2004.

[3] J. Kim and J. S. Lai, "Quad sampling incremental inductance measurement through current loop for switched reluctance motor," *IEEE Trans. Instrum. Meas.*, vol. 69, no. 7, pp. 4251–4257, Jul. 2020,

[4] X. Liu and Z. Q. Zhu, "Electromagnetic performance of novel variable flux reluctance machines with DC-field coil in stator," *IEEE Trans. Magn.*, vol. 49, no. 6, pp. 3020–3028, Jun. 2013.

[5] Z. Q. Zhu, B. Lee, and X. Liu, "Integrated field and armature current control strategy for variable flux reluctance machine using open winding," *IEEE Trans. Ind. Appl.*, vol. 52, no. 2, pp. 1519–1529, Apr. 2016.

[6] X. Liu and Z. Q. Zhu, "Comparative study of novel variable flux reluctance machines with doubly fed doubly salient machines," *IEEE Trans. Magn.*, vol. 49, no. 7, pp. 3020–3028, Jul. 2013.

[7] M. Gyimesi and D. Ostergaard, "Inductance computation by incremental finite element analysis," *IEEE Trans. Magn.*, vol. 35, no. 3, pp. 1119–1122, May 1999.

[8] K. J. W. Pluk, J. W. Jansen, and E. A. Lomonova, "Hybrid analytical modeling: Fourier modeling combined with mesh-based magnetic equivalent circuits," *IEEE Trans. Magn.*, vol. 51, no. 8, pp. 1–12, Aug. 2015.

[9] M. Desvaux, S. Sire, S. Hlioui, H. Ben Ahmed, and B. Multon, "Development of a hybrid analytical model for a fast computation of magnetic losses and optimization of coaxial magnetic gears," *IEEE Trans. Energy Convers.*, vol. 34, no. 1, pp. 25–35, Mar. 2019.

[10] P. Zhou, D. Lin, C. Lu, M. Rosu, and D. M. Ionel, "An adaptive fixed-point iteration algorithm for finite-element analysis with magnetic hysteresis materials," *IEEE Trans. Magn.*, vol. 53, no. 10, pp. 1–5, Oct. 2017.

[11] L. A. J. Friedrich, M. Curti, B. L. J. Gysen, and E. A. Lomonova, "High-order methods applied to nonlinear magnetostatic problems," *Math. Comput. Appl.*, vol. 24, no. 19, pp. 1–15, Jan. 2019.

[12] S. Ouagued, Y. Amara, and G. Barakat, "Cogging force analysis of linear permanent magnet machines using a hybrid analytical model," *IEEE Trans. Magn.*, vol. 52, no. 7, pp. 1–4, Jul. 2016.

[13] J. Bao, B. L. J. Gysen, and E. A. Lomonova, "Hybrid analytical modeling of saturated linear and rotary electrical machines: Integration of Fourier modeling and magnetic equivalent circuits," *IEEE Trans. Magn.*, vol. 54, no. 11, pp. 1–5, Nov. 2018.

Authorized licensed use limited to: Eindhoven University of Technology. Downloaded on September 01,2021 at 08:01:42 UTC from IEEE Xplore. Restrictions apply.